DTU Library

Raman Spectroscopy of Conformational Changes in Membrane-Bound Sodium Potassium ATPase

Helix Nielsen, Claus; Abdali, Salim; Lundbæk, Jens August; Cornelius, Flemming

Link back to DTU Orbit

Raman Spectroscopy of Conformational Changes in Membrane-Bound Sodium Potassium ATPase

In this investigation we assess the potential of Raman spectroscopy as a tool for probing conformational changes in membrane-spanning proteins – in this case, the sodium potassium adenosine triphosphatase (Na^+,K^+-ATPase). Spectral analysis of protein-lipid complexes is complicated by the presence of a lipidic environment, rendering the amide I spectral region difficult to analyze. We have therefore focused on spectral changes in the disulfide region arising from cysteine (Cys) cross-linking and the tyrosine (Tyr) Fermi doublet region arising from changes in Tyr hydrogen bonding environment. Specifically, we have studied the conformational changes in the Na^+,K^+-ATPase undergoing the $E_2 \rightarrow E_1$ transition as controlled by Na^+. These conformational changes were compared to the E_1 conformation stabilized by controlled proteolytic digestion. Our results show that controlled digestion promoting the E_1 conformation leads to changes in cross-linking between Cys residues as well as changes in the Tyr hydrogen bonding environment. In contrast, Na^+ binding, which also promotes the E_1 conformation, does not lead to any changes in these spectral regions. This demonstrates that the functional E_1 state of the Na^+,K^+-ATPase stabilized by N-terminal truncation differs from that induced by Na^+ binding, and that the N-terminal truncation leads to changes in protein structure that affect the average hydrophobic environment of protein Tyr, possibly reflecting changes in the hydrophobic coupling between protein and membrane. This illustrates the stabilizing role of the N-terminal domain under physiological conditions. More generally, it shows that Raman spectroscopy might be a useful tool in understanding the relationship between functional states and structural changes in membrane-bound proteins.

Claus Hélix Nielsen, Salim Abdali, Jens August Lundbæk, and Flemming Cornelius

S odium potassium adenosine triphosphatase (Na^+,K^+-ATPase) is a transmembrane protein enzyme member of the P-type ATPase family (1). The minimal functional unit consists of an α-subunit of about 100 kDa and a β-subunit of about 38 kDa (2). The enzyme acts as an electrogenic ion transporter in the plasma membrane of all mammalian cells (3). Each reaction cycle of the Na^+,K^+-ATPase activity pumps three sodium ions out from the cell in exchange
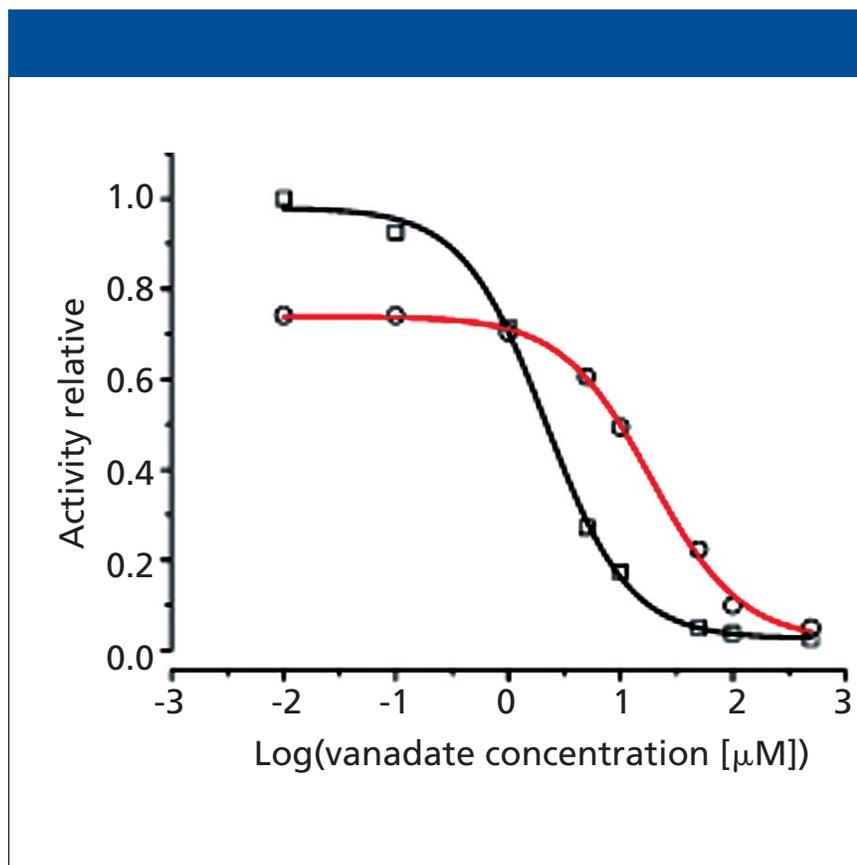
Figure 1: Vanadate sensitivity of Na+,K+-ATPase. ATP hydrolysis was measured in 120 mM Na+, 10 mM K+, 2 mM Mg^{2+}, and 1 mM ATP at 23 °C using the method of Baginski (52) as described in Materials and Methods. Data are presented as fractions of the activity in the absence of vanadate as mean $\pm$ SD ($n = 3$). The curves are fit using a one site competition (Hill) model with $K_{0.5}$ and n_H as free parameters. Effects of tryptic cleavage: control: $K_{0.5} = 2.2$ μM and $n_H = -1.13$ $\pm$ 0.05 (black); after trypsin treatment: $K_{0.5} = 18.3$ μM and $n_H = -1.11 \pm 0.06$ (red); the two values being significantly different with $p < 0.0001$.

for two potassium ions under hydrolysis of one molecule of adenosine triphosphate (ATP). The primary role of Na+,K+-ATPase is to maintain a low intracellular sodium concentration and a high intracellular potassium concentration. In addition to its pumping activity, the enzyme also has been suggested to function as a signal-transducing receptor for cardiotonic steroids (4–6).

Most reaction schemes of Na+,K+-ATPase are based upon the original Albers–Post mechanism (7,8) involving phosphorylated and dephosphorylated forms of the enzyme, both undergoing conformational transitions ($E_1P \rightarrow E_2P$ and $E_2 \rightarrow E_1$) coupled to ion translocation steps (for recent reviews, see references 9 and 10). In the E_1 conformation, the enzyme has a high affinity for ATP

and binds three cytoplasmic Na+ ions. In connection with a phosphorylation reaction in which a conserved aspartate residue in the enzyme is phosphorylated to form a high-energy phosphoenzyme (E_1P), three Na+ ions are occluded. This is followed by a spontaneous transition to a low-energy E_2P form and translocation of Na+ across the membrane. Two K+ ions are then bound at the extracellular side and become occluded by a dephosphorylation of the enzyme. Finally, low-affinity binding of ATP deoccludes and translocates the two K+ ions. Under physiological conditions, the $E_2 \rightarrow E_1$ transition is part of the pumping cycle and induced by the presence of Na+.

The first biochemical evidence for structural changes between E_1 and E_2

came from tryptic digestion experiments using renal Na+,K+-ATPase (11). In the absence of other ligands than K+ (that is, in E_2), trypsin cleaves at arginine-438 (Arg-438) (T1) and subsequently at lysine-30 (Lys-30) (T2) in the N-terminal part of the α-subunit. In the presence of Na+ (that is, in E_1), T1 is protected against trypsin, while T2 is cleaved rapidly followed by a slower cleavage at Arg-262 (T3). Specific cleavage at T2, whereby the first 30 amino acids are removed (N-terminal truncation), stabilizes the enzyme in the E_1 conformation and decreases hydrolytic capacity (V_{max}) (11).

The N-terminal region contains a lysine-rich cluster and is among the most diverse within P-type ATPases, even between Na+,K+-ATPase isoforms, and has been assigned special functional significance. Thus, in a series of papers, Rhoda Blostein and colleagues (12,13) proposed an autoregulatory role for the N-terminus, which controls the E_1/E_2 conformational equilibrium by interdomain interactions between the cytoplasmic TM2-3 and TM4-5 domains. Recently, the N-terminus also has been implicated in the tissue-specific regulation of Na+,K+-ATPase by associated FXYD-proteins (13).

Unfortunately, a homologous region to the N-terminus of Na+,K+-ATPase is missing in the sarco(endo)plasmic reticulum Ca^{2+}-ATPase (SERCA), another member of the P-type ATPases, for which structures have been solved at the molecular level in several different E_1 and E_2 conformations stabilized by various ligands (14–19). Key features of these structures are thought to be shared by other P-type ATPases (20). One important feature of the SERCA 3D structure is the existence of three main cytoplasmic domains: the nucleotide-binding N-domain, the phosphorylation or P-domain, and the actuator, or A-domain where the N-terminal portion of the A-domain consists of two short helices and an extension connecting to TM1. Similar structures are assumed in the Na+,K+-ATPase, but with an additional third N-terminal helical segment containing the T2 trypsin digestion site (13,21). Thus, we cannot infer structural consequences of N-terminal
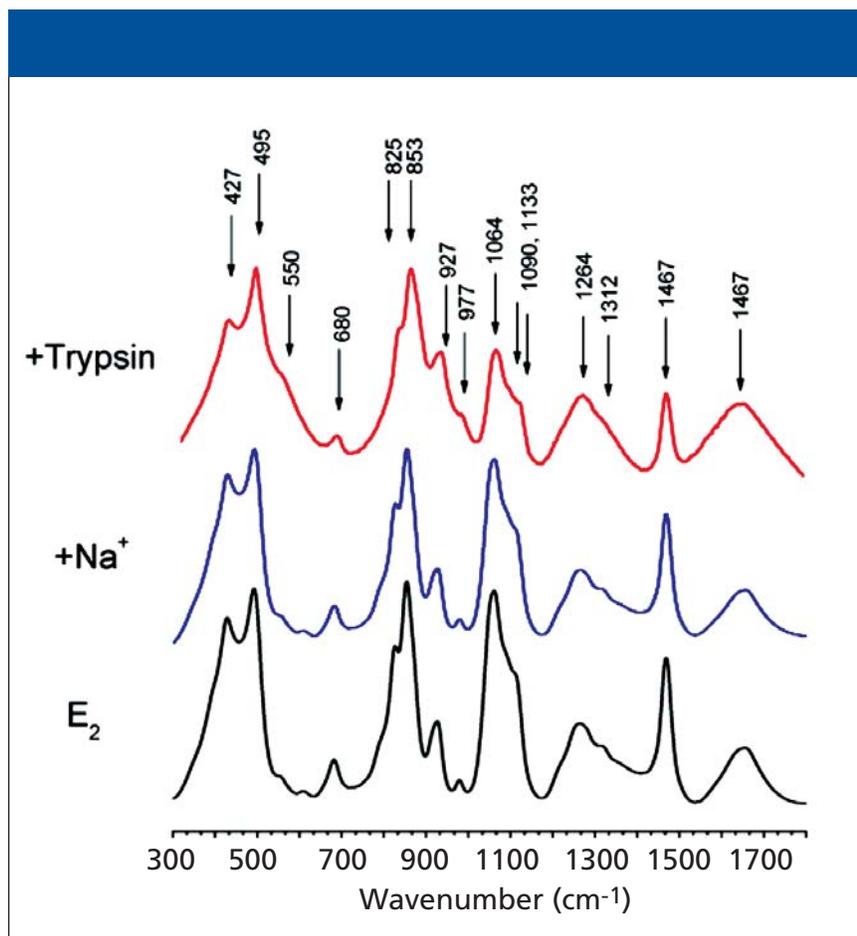
Figure 2: Stacked Raman spectra of the Na$^+$,K$^+$-ATPase in the 300–1550 cm^{-1} region. (E$_2$): in the E$_2$ promoting buffer; (black); after tryptic digestion (red); and binding of Na$^+$ (blue). All spectra represent the average intensity from 60 scans with each 10-s illumination time and 1024 spectral sample points. For band assignments, see text.

truncation from homology modeling to the crystal structures of SERCA. It therefore becomes important to see if we can use other tools for analyzing the role of the N-terminal on the structural organization of the Na$^+$,K$^+$-ATPase.

Raman spectroscopy has been used to monitor the changes of secondary structure in the Na$^+$,K$^+$-ATPase (the E$_2$→E$_1$ transition induced by changes in the concentration of Na$^+$ and K$^+$) occurring in the amide I region (22,23), but with conflicting results. Nabiev and colleagues (22) associated the E$_1$→E$_2$ transition with an increase in α-helical content of about 10%, whereas Anzenbacher and colleagues (23) found a decrease in α-helical content of less than 10%. The problem that arises when using the amide I region analysis of membrane-bound proteins is that this region typically shows a broad spectrum that contains several spectral contributions from both protein and lipid components (24). Various subtraction procedures can be applied in order to separate out these components. These procedures will all significantly influence the experimental data, but it is not clear to what extent they can produce results from which unambiguous quantitative conclusions about structural changes can be drawn (23). Also, integral membrane proteins undergoing a conformational change are likely to perturb the surrounding lipid bilayer, because the sequence of conformational state change might involve changes in protein structure that affect the protein–lipid boundary (25–28), further complicating interpretation of the amide I region.

In this study, we have therefore investigated whether other Raman spectral markers than the amide I region can be used to trace the E$_1$→E$_2$ transition without subtraction of lipid and buffer signals. We have focused on markers that can be assigned to changes in the protein only and not to eventual changes in the lipid environment. Specifically, we have investigated changes in disulfide bond-stretching vibrations and the Fermi doublet of tyrosine in shark rectal gland Na$^+$,K$^+$-ATPase.

Disulfide bonds play a critical role in the folding of many proteins and in the stabilization of tertiary structures (29). By threading the rat Na$^+$,K$^+$-ATPase sequence onto the crystal structure of the closely related skeletal-muscle sarcoplasmic recticulum Ca^{2+} ATPase (SERCA) structure (14), several cross-linking cysteine (Cys) sites have been proposed for the rat Na$^+$,K$^+$-ATPase (20). A gapped Blast alignment reveals that all Cys residues in the α-subunit of rat Na$^+$,K$^+$-ATPase (NP 036636) are conserved in the shark rectal gland Na$^+$,K$^+$-ATPase α-subunit (CAG77578) investigated here (results not shown). Raman markers have been described for the S-S stretching (ν_{SS}) (30,31) and C-S stretching (ν_{CS}) modes (32,33) in the 500 to 700 cm^{-1} region, and we investigate possible changes in this region.

We also have investigated Tyr hydrogen bonding environment in E$_1$ and E$_2$ conformers because the shark rectal gland Na$^+$,K$^+$-ATPase sequence contains 25 Tyr residues. Tyr gives rise to a Fermi doublet at 825 cm^{-1} and 853 cm^{-1}, and the intensity ratio I_{853}/I_{825} of the doublet represents the average protonation state (whether Tyr is an acceptor or donor for hydrogen bonds) (24). We use 5% glycerol to stabilize protein function (see Materials and Methods); because glycerol has a Raman band (C-C stretch) at 852 cm^{-1} (34), we cannot use the ratio I_{853}/I_{825} to quantify the average strength of the hydrogen-bonding environment directly for the tyrosine residues of Na$^+$,K$^+$-ATPase. Nevertheless, we will use the I_{853}/I_{825} ratio to qualitatively monitor possible changes associated with the E$_2$→E$_1$ transition.

In the present investigation, we have compared cation-induced E$_1$ and E$_2$ conformations by Raman spectroscopy to the conformational changes found by

N-terminal truncation of the shark Na^+,K^+-ATPase. We used incubation with a K^+ free histidine–glycerol buffer (35,36) as a reference for the enzyme being in the E_2 state because glycerol stabilizes the E_2 conformation (37–40) and preserves activity (41). We then rapidly incubated with excess Na^+ to induce the transition to E_1 as previously described (42). Finally, we used controlled tryptic digestion with exposure of the T2 cleavage site to stabilize the enzyme in the E_1 state (43). We assessed the steady-state distribution of E_1 and E_2 using enzyme sensitivity to inhibition by vanadate, a transition state analog of inorganic phosphate that binds preferentially with the E_2 conformer of the enzyme (44–46). In the following, we first show inhibition to vanadate to demonstrate the expected change in the E_1/E_2 equilibrium before and after tryptic digestion. Then we assign the E_2 Raman spectrum. Finally, we investigate whether spectral changes induced by tryptic digestion or Na^+ binding are observable as changes in the 400–700 cm^{-1} disulfide bond-stretching spectral region and the Tyr 850/830 cm^{-1} doublet bands.

Materials and Methods

Enzyme preparation

Membrane-bound Na^+,K^+-ATPase (EC 3.6.1.37) from rectal glands of the shark *Squalus acanthias* (α-subunit nucleotide sequence number AJ781093) was prepared as previously described (47). This involves isolation of well-defined membrane fragments by differential centrifugation following treatment of microsomes with low concentrations (~0.15%) of deoxycholate to remove loosely attached proteins. The final protein:lipid ratio is about 1:1 (wt/wt), and the specific ATPase activity at 37 °C and pH 7.4 was measured according to Ottolenghi (48) to be 1617 μmol/mg/h. The protein stock concentration was determined to be 4.943 mg/mL according to the Peterson modification of the Lowry method using bovine serum albumin as a standard (49,50). The stock concentrations were diluted into 1 mg/mL aliquot samples before the experiments.

For all experiments, the starting conformation E_2 was induced using a buffer with 30 mM histidine and 5% glycerol at pH 6.8. E_2 samples (1-mL aliquot) were kept at –20 °C and were brought to room temperature (23 °C) before further manipulations and measurements took place. In the tryptic digestion experiments, the E_1 conformation was induced using N-terminal truncation of the α-subunit (43). The membrane-bound enzyme was incubated with trypsin (T-1426, Sigma, St. Louis, Missouri) at a trypsin:protein ratio of 1:20 (wt/wt) for 10 min on ice in the presence of 20 mM histidine, 130 mM NaCl, and 1 mM EDTA at pH 7.0. Then, trypsin inhibitor was added at 1:10 (wt/wt) (Sigma) as previously described (51) followed by washing and resuspension. In the ion-binding experiments, the E_1 conformation was introduced by addition of 30 mM NaCl to the membrane-bound enzyme in histidine-glycerol buffer, resulting in a rapid transition to the $E_1(Na^+)_3$ state (42).

Spectra were recorded independently at least three times for each type of experiment. The vanadate sensitivity of

Na^+,K^+-ATPase activity was measured in 120 mM Na^+, 10 mM K^+, 2 mM Mg^{2+}, and 1 mM ATP at 23 °C, as previously described (13). For all experiments, hydrolytic activity was checked before and after Raman measurements at 23 °C in 130 mM Na^+, 20mM K^+, 4 mM Mg^{2+}, and 3 mM ATP in 15 mM histidine (pH 7.4) using the method of Baginski and colleagues (52).

Raman Spectroscopy

Raman spectra were recorded using ChiralRaman Instrument (BioTools, Wauconda, Illinois), which utilizes a 532-nm solid-state *cw* laser source (Excel, QuantumLaser, UK), and the charge-coupled device (CCD) camera mounted on the system is optimized to spectral detection between 100 and 2400 cm^{-1}. The resolution of the ChiralRaman is approximately 5 cm^{-1}, determined by the width of the individual fibers in the fiber-optic cable at the entrance to the spectrograph (53). The instrument simultaneously provides Raman and Raman optical activity (ROA) spectra; however, in this study, we made use of only the Raman spectra. The enzyme sample was placed in a 120-μL quartz cell, and accumulated spectra were recorded at 100-mW laser intensity. The entire recording took 30 min per sample, corresponding to 180 scans each with 10 s illumination time followed by 1.5 s darkness. This ensured negligible induction of heat in the sample (measured to < 0.1 °C). The Raman spectra were baseline corrected and displayed using OriginPro 7.5 (OriginLab, Northampton, Massachusetts).

Results

E_1/E_2 Equilibrium After Controlled Tryptic Digestion

Orthovanadate is a transition homolog of inorganic phosphate that binds to the E_2 conformation of the Na^+,K^+-ATPase (44); thus, sensitivity to inhibition by vanadate can be used as a measure of the steady-state distribution between the E_2 and E_1 conformations (21,46). Figure 1 shows the vanadate sensitivity of the Na^+,K^+-ATPase after tryptic digestion. After tryptic digestion, the vanadate inhibition constant $K_{0.5}$ increased from about 2.2 μM to about 18 μM (*p* <
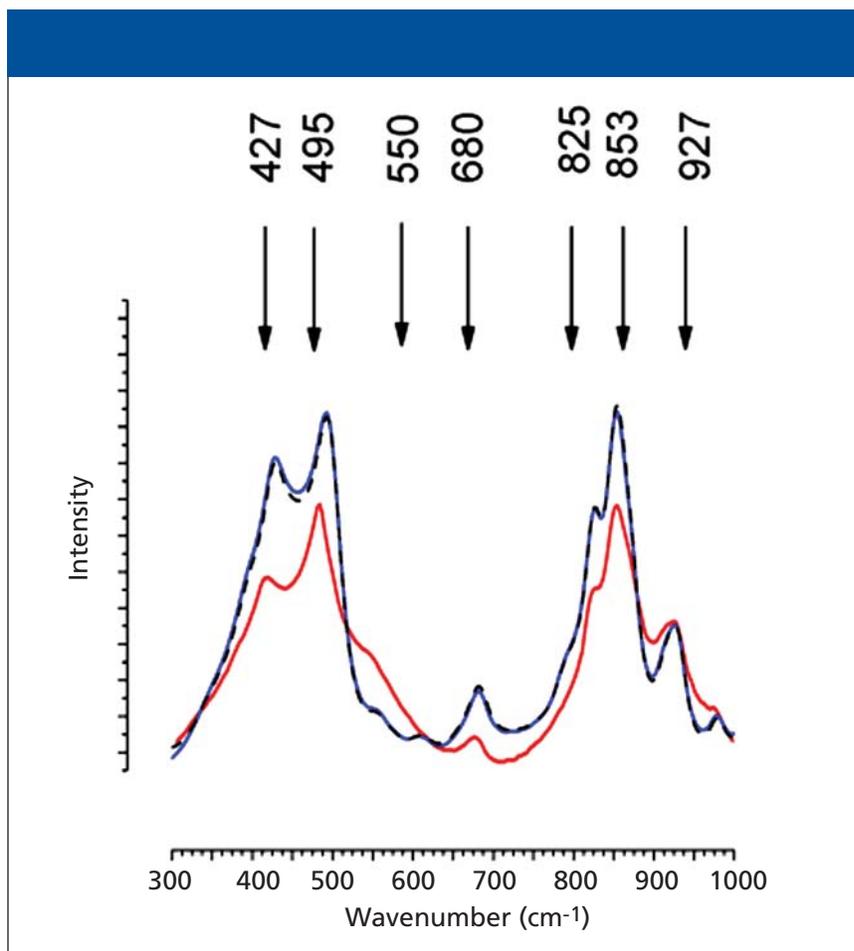

Figure 3: Overlayed spectra of the disulfide bond vibrational region and Tyr Fermi doublet region of the Na^+,K^+-ATPase after tryptic digestion (red) and binding of Na^+ (blue), together with the control E_2 spectrum (black).

0.001). This demonstrates that tryptic digestion decreases sensitivity to vanadate inhibition and thus shifts the E_2/E_1 equilibrium toward E_1.

In order to assess whether these proteolytically induced conformational changes and changes due to ion binding are reflected in the vibrational Raman spectra, we first describe the reference E_2 spectrum; then we proceed to analyze the spectral changes associated with the induced $E_2 \rightarrow E_1$ transitions.

Band Assignment of the Reference E_2 Spectrum

Raman spectra of Na^+,K^+-ATPase in the E_2 promoting buffer (hereafter referred to as the E_2 comformer) were recorded (the spectrum labeled E_2 in Figure 2) and contain spectral markers from the membrane fragments and embedded protein

as well as buffer (mainly from buffer glycerol, because H_2O solutions of histidine do not show clear Raman bands in the considered region (300–1650 cm^{-1}) (54). The intensity variation between different experiments prepared under the same conditions was < 5%. This was estimated by scaling spectra obtained from different samples using the glycerol peak at 927 cm^{-1} (34) as scaling reference because this peak has minimal contribution from the protein (23,55).

In addition to the 927-cm^{-1} glycerol peak, several other glycerol bands are known in the 300–1560 cm^{-1} region (34) and, to some extent, these bands overlap with bands arising from the protein as well as the membrane fragments. Thus, the following assignment will be based upon known protein (Na^+,K^+-

ATPase) and lipid bands (23,24) as well as known glycerol bands (34).

The 400–500 cm^{-1} region is characterized by two distinguishable peaks at 427 and 495 cm^{-1} and a shoulder around 550 cm^{-1}. The 427-cm^{-1} peak can be assigned to a glycerol COO rock vibration (34). We assign the 495-cm^{-1} band as resulting from a combination of the 510-cm^{-1} vibration from spontaneously formed protein disulfide bonds (56) in the form of *gauche-gauche-gauche* bonds (24,57) and a glycerol COO rock vibration at 485 cm^{-1} (34). The 550-cm^{-1} shoulder can be assigned to protein S-S bonds in *trans-gauche-trans* configurations (57).

A peak at 680 cm^{-1} can be attributed to C-S stretch vibration (58); the peaks at 825 cm^{-1} and 853 cm^{-1} represent Tyr Fermi doublet arising from a resonance between the ring-breathing vibration and the overtone of the out-of-plane ring bend vibration of the para-substituted phenyl ring in Tyr. There is also a glycerol band known to be at 852 cm^{-1} (34) and the ratio $I_{853}/I_{825} = 1.36$.

The peaks at 927 cm^{-1} and 977 cm^{-1} can be assigned to glycerol vibrations, and the skeletal optical region between 1000 cm^{-1} and 1150 cm^{-1} is characterized by a peak at 1060 cm^{-1} accompanied by a shoulder extending up to 1150 cm^{-1}. The vibrational modes in this region are highly sensitive to hydrocarbon (lipid) state (59) and the presence of glycerol (34,60–62). Three lipid bands contribute to this region (62): the 1064 and 1133 cm^{-1} characteristic of all trans acyl chain segments, and one at 1090 cm^{-1} arising from acyl chains containing gauche configurations with a symmetric O-P-O stretching band arising from lipid headgroup phosphate groups superimposed. However, the presence of protein-diffuse C-C stretching as well as glycerol bands (34) in the 1000–1150 cm^{-1} region prevents a quantitative analysis of this region.

In addition to the skeletal optical region lipid bands, the amide III band at 1260 cm^{-1} with a shoulder at 1312 cm^{-1} and the strong band at 1467 cm^{-1} can be assigned to CH$_2$ deformations of the lipids in the membrane fraction (63) as well as buffer glycerol (34). Although the amide III region (C-N stretching) in

principle contains quantitative information about secondary structure (such as the ratio between α-helical and β-sheet content), we will not analyze it here due to the prominent lipid and glycerol components in our samples and the ensuing problems in quantitatively separating out the protein signal components in those bands. We also disregard the amide I region (C=O stretching) in spite of the spectral difference between E$_2$ and E$_1$ induced by tryptic digestion (Figure 2).

We note the absence of a phenylalanine band at 1003 cm^{-1} typically present in protein spectra. However, this band depends upon protein conformation and might not be visible generally, as reported for rhodopsin (64).

Disulfide bonds play a critical role in the folding of many proteins and in the stabilization of tertiary structures.

Changes in Disulfide Vibrational Bands and Tyr Fermi Doublet Bands Associated with the E$_2$→E$_1$ Transition After Either Tryptic Digestion or Ion Binding
In our analysis of changes in the Raman spectrum upon inducing E$_2$→E$_1$ transitions, we will assume that the buffer glycerol bands are not affected by any conformational change in the protein per se. Figure 2 shows the stacked spectra after tryptic digestion and sodium binding, together with the E$_2$ spectrum. The tryptic digestion Raman intensities are lower than those of the control and the Na$^+$ incubated samples due to wash and resuspension. To compare the disulfide and Tyr spectral regions from the tryptic digestion and sodium binding experiments, we use the glycerol peak at 927 cm^{-1} (65) as a scaling reference. Figure 3 shows the scaled and superimposed spectra between 300 cm^{-1} and 1000 cm^{-1}. Tryptic digestion results in increased intensity between 500 cm^{-1} and 650 cm^{-1} as compared with the E$_2$

spectrum: the 427-cm^{-1} and 495-cm^{-1} peak intensities are both decreased and broadened and the shoulder around 550 cm^{-1} is more pronounced. This shoulder is due to the S-S *trans-gauche-trans* configurations of the CβS-S′-Cβ′ disulfide bridges (30,66). The C-S stretching at 680 cm^{-1} is decreased and the intensity ratio I_{850}/I_{830} corresponding to the Tyr Fermi doublet is increased after tryptic digestion: $I_{850}/I_{830} = 1.43$, mirroring the changes in vanadate sensitivity (Figure 1). In contrast to the spectrum obtained upon tryptic digestion, the addition of Na$^+$ does not reveal any detectable change in the spectrum.

Discussion

The original distinction between E$_1$ and E$_2$ was based upon the proposal that one had cation sites facing the cytoplasm and the other facing the exterior (7,8). The first direct evidence for two forms of the dephosphorylated enzyme came from divergent responses to digestion of the enzyme by trypsin (43). Clearly, there are three cleavage sites and the rate of hydrolysis is a function of the ionic environment as would be expected if Na$^+$ and K$^+$ stabilized alternative conformations of the enzyme. In the Na$^+$,K$^+$-ATPase, the E$_2$→E$_1$ transition is rate-limiting for subsequent steps in the pump cycle (38), and it is therefore of special interest to investigate structural changes associated with this transition in the Na$^+$,K$^+$-ATPase pump cycle.

Previous spectroscopic studies have investigated the structural changes associated with Na$^+$-induced E$_2$→E$_1$ transition using circular dicroism (67,68), infrared spectroscopy (69), and Raman spectroscopy (22,23) with contradictory results. Our study shows that no disulfide bridges are formed nor does the average Tyr hydrophobic environment change upon binding of Na$^+$. Thus, the Na$^+$-induced E$_1$ form is not associated with an increased number of covalent intrasubunit bonds or with large changes in protein secondary structure compared with the E$_2$ structure. This is not in contrast to the fact that the protein does undergo conformational changes upon ion binding; rather, the results support that this is associated with rotation of protein domains around few hinge

amino acids with very little secondary structural changes (10). Indeed, it has recently been suggested that a compact arrangement of the three cytoplasmic domains in SERCA is maintained during the reaction cycle, and that the $E_2 \rightarrow E_1$ transition must be regarded as an equilibrium between two compact states, where the N-domain and A-domain is not far detached from the P-domain (15). Thus, in the E_1 conformation, the N-domain docks onto the P-domain and the A-domain is rotated 45° upward, whereas in the E_2 conformation, the A-domain rotates back and docks onto the P-domain, whereby the N-domain is slightly displaced.

In SERCA, a key role in controlling the $E_2 \rightarrow E_1$ transition is ascribed to the A-domain, which includes the N-terminus and encompasses the three first transmembrane helical segments. The most clear place where the SERCA and the Na^+,K^+-ATPase sequences differ is at the N-terminus, and the initial 30 amino acids of Na^+,K^+-ATPase are absent in SERCA. Also, within Na^+,K^+-ATPase isoforms the N-terminal sequence homology is low. Indeed, several investigations have demonstrated specific functional significance of the Na^+,K^+-ATPase N-terminal domain. Originally, Jørgensen and colleagues (11,70,71) demonstrated that trypsin cleavage at T2 of the enzyme in the presence of Na^+ stabilized the E_1 conformation, reduced the catalytic capacity, and decreased the K^+-sensitivity of the dephosphorylation reaction. Others have demonstrated effects on cation translocation (72) and transport stoichiometry (73). Subsequently, Blostein's group (12,21) used deletion mutants and isoforms chimeras to investigate the structural basis for these effects and proposed an autoregulatory role for the N-terminus in controlling interdomain interaction between the A-domain and the large cytoplasmic TM4/5 domain. Recently, we have demonstrated the species specificity of this interaction and suggested interaction of the N-terminus with the FXYD regulatory proteins (13). Nevertheless, we still miss structural information as to the spatial interaction of the N-terminus with the rest of the α-subunit, especially because we cannot relate this domain to the crystal structure of SERCA.

It was, therefore, interesting to see whether we could monitor changes in the Raman spectra associated with N-terminal truncation of the Na^+,K^+-ATPase. In the experiments with controlled tryptic digestion, we see a 10-fold decrease in vanadate sensitivity (Figure 1), indicating E_1 stabilization, together with a marked increase in Raman intensity at 550 cm^{-1}. This indicates that disulfide bridges are formed when the E_1 conformation is stabilized by tryptic digestion. The fact that disulfide crosslinks are formed after cleavage at the T2 site indicates modifications in the 3D packing induced by proteolysis and is in line with the findings that proteolytic fragments of transmembrane spans (74) cross-link only after diges-

> *Raman spectroscopy might be a useful tool in label-free dissection of protein conformational changes in lipid–protein complexes.*

tion (75). Also, the average Tyr hydrogen bonding is changed. I_{850}/I_{830} increases, and although we cannot assess directly the protonation state of the 25 tyrosine residues due to the glycerol peak, an increase in I_{850}/I_{830} can be associated with an increased exposure of Tyr residues to the aqueous surroundings. Mapping the 25 Tyr residues onto the SERCA structure reveals a distribution with about one half of the Tyr residues in the interfacial regions of the transmembrane segments and the other half distributed in the cytoplasmic regions. In principle, any change in Tyr exposure could be due to changes in either group of Tyr residues; based upon analogy with SERCA conformational changes, it is most likely that changes in I_{850}/I_{830} reflect changes in the transmembrane Tyr exposure to the aqueous phase, because the secondary structure of the cytoplasmic regions appears unaltered

in SERCA upon Ca^{2+} binding (16). Thus, the formation of disulfide bonds induces changes in overall protein structure — possibly reflecting changes in the hydrophobic interaction between membrane and protein.

Interestingly, the spectral changes observed after N-terminal truncation, which stabilizes the E_1 conformation, seem to result in more profound structural changes than the $E_2 \rightarrow E_1$ conformational change induced by Na^+ binding. Indeed, this might be a result of a perturbed molecular arrangement induced by proteolysis, reflecting the stabilization induced by the N-terminal domain under physiological conditions. In this connection, it is worth emphasizing the autoregulatory function of the lysine-rich N-terminus, which is proposed to take place by interaction of the TM2/3 loop of the A-domain with the cytoplasmic TM4/5 catalytic loop as controlled by the N-terminus (21).

Taken together, our results show that the biochemically defined E_1 state of Na^+,K^+-ATPase does not represent a unique structural conformation; rather, the conformation depends upon how the state is introduced. Specifically, our results demonstrate that N-terminal truncation leads to changes in protein structure that affect the average hydrophobic environment of protein Tyr residues, possibly reflecting changes in the hydrophobic coupling between protein and membrane. This illustrates the stabilizing role of the N-terminal domain under physiological conditions. More generally, our studies demonstrate that Raman spectroscopy might be a useful tool in label-free dissection of protein conformational changes in lipid–protein complexes.

References

(1) J.V. Moller, B. Juul, and M. le Maire,

Biochim. Biophys. Acta **1286**, 1–51 (1996).

(2) J.C. Skou, *Methods Enzymol.* **156**, 1–25 (1988).

(3) P.L. Jorgensen, K.O. Hakansson, and S.J. Karlish, *Annu. Rev. Physiol.* **65**, 817–849 (2003).

(4) P. Kometiani, J. Li, L. Gnudi, B.B. Kahn, A. Askari, and Z. Xie, *J. Biol. Chem.* **273**, 15249–15256 (1998).

(5) P. Kometiani, L. Liu, and A. Askari, *Mol. Pharmacol.* **67**, 929–936 (2005).

(6) K. Mohammadi, L. Liu, J. Tian, P. Kometiani, Z. Xie, and A. Askari, *J. Cardiovasc. Pharmacol.* **41**, 609–614 (2003).

(7) R.L. Post, S. Kume, T. Tobin, B. Ocutt, and A.K. Sen, *J. Gen. Physiol.* **54**, 306–326 (1969).

(8) R.W. Albers, *Annu. Rev. Biochem.* **36**, 727–756 (1967).

(9) H.J. Apell, *Bioelectrochemistry* **63**, 149–156 (2004).

(10) J.D. Horisberger, *Physiology (Bethesda)* **19**, 377–387 (2004).

(11) P.L. Jorgensen, *Biochim. Biophys. Acta* **694**, 27–68 (1982).

(12) L. Segall, L.K. Lane, and R. Blostein, *Ann. N.Y. Acad. Sci.* **986**, 58–62 (2003).

(13) F. Cornelius, Y.A. Mahmmoud, L. Meischke, and G. Cramb, *Biochemistry* **44**, 13051–13062 (2005).

(14) C. Toyoshima, M. Nakasako, H. Nomura, and H. Ogawa, *Nature* **405**, 647–655 (2000).

(15) A.M. Jensen, T.L. Sorensen, C. Olesen, J.V. Moller, and P. Nissen, *EMBO J.* **25**, 2305–2314 (2006).

(16) C. Toyoshima and H. Nomura, *Nature* **418**, 605–611 (2002).

(17) C. Toyoshima and T. Mizutani, *Nature* **430**, 529–535 (2004).

(18) C. Toyoshima, H. Nomura, and T. Tsuda, *Nature* **432**, 361–368 (2004).

(19) T.L. Sorensen, J.V. Moller, and P. Nissen, *Science* **304**, 1672–1675 (2004).

(20) K.J. Sweadner and C. Donnet, *Biochem. J.* **356**, 685–704 (2001).

(21) L. Segall, L.K. Lane, and R. Blostein, *J. Biol. Chem.* **277**, 35202–35209 (2002).

(22) I.R. Nabiev, K.N. Dzhandzhugazyan, R.G. Efremov, and N.N. Modyanov, *FEBS Lett.* **236**, 235–239 (1988).

(23) P. Anzenbacher, P. Mojzes, V. Baumruk, and E. Amler, *FEBS Lett.* **312**, 80–82 (1992).

(24) A.T. Tu, AT. *Spectroscopy of Biological Systems* (Clark, R.J.H., Hester, R.E. Eds.) Wiley: 47–112 (Abstr.) (1986).

(25) C. Nielsen, M. Goulian, and O.S. Andersen, *Biophys. J.* **74**, 1966–1983 (1998).

(26) P.N.T. Unwin and P.D. Ennis, *Nature* **307**, 609–613 (1984).

(27) M.O. Jensen and O.G. Mouritsen, *Biochim. Biophys. Acta* **1666**, 205–226 (2004).

(28) N. Unwin, C. Toyoshima, and E. Kubalek, *J. Cell Biol.* **107**, 1123–1138 (1988).

(29) C.B. Anfinsen and H.A. Scheraga, *Adv. Protein Chem.* **29**, 205–300 (1975).

(30) H. Sugeta, A. Go, and T. Miyazawa, *Chem. Lett.* **1**, 83–86 (1972).

(31) H. Sugeta, A. Go, and T. Miyazawa, *Bull. Chem. Soc. Jpn.* **48**, 3407–3411 (1975).

(32) N. Nogami, H. Sugeta, and T. Miyazawa, *Bull. Chem. Soc. Jpn.* **48**, 3573–3575 (1975).

(33) N. Nogami, H. Sugeta, and T. Miyazawa, *Bull. Chem. Soc. Jpn.* **48**, 2417–2420 (1975).

Circle 36

(34) E. Mendelovici, R.L. Frost, and T. Kloprogge, *J. Raman Spectrosc.* **31**, 1121–1126 (2000).

(35) S.J. Karlish and D.W. Yates, *Biochim. Biophys. Acta* **527**, 115–130 (1978).

(36) S.J. Karlish, *J. Bioenerg. Biomembr.* **12**, 111–136 (1980).

(37) M. Esmann, J.C. Skou, and C. Christiansen, *Biochim. Biophys. Acta* **567**, 410–420 (1979).

(38) C. Lupfert, E. Grell, V. Pintschovius, H.J. Apell, F. Cornelius, and R.J. Clarke, *Biophys. J.* **81**, 2069–2081 (2001).

(39) F.M. Schuurmans Stekhoven, H.G. Swarts, J.J. de Pont, and S.L. Bonting, *Biochim. Biophys. Acta* **815**, 16–24 (1985).

(40) F.M. Schuurmans Stekhoven, H.G. Swarts, G.K. Lam, Y.S. Zou, and J.J. De Pont, *Biochim. Biophys. Acta* **937**, 161–176 (1988).

(41) D. Thoenges, C. Zscherp, E. Grell, and A. Barth, *Biopolymers* **67**, 271–274 (2002).

(42) J.C. Skou and M. Esmann, *Biochim. Biophys. Acta* **746**, 101–113 (1983).

(43) P.L. Jorgensen, *Biochim. Biophys. Acta* **401**, 399–415 (1975).

(44) L.C. Cantley, Jr, L.G. Cantley, and L. Josephson, *J. Biol. Chem.* **253**, 7361–7368 (1978).

(45) N. Boxenbaum, S.E. Daly, Z.Z. Javaid, L.K. Lane, and R. Blostein, *J. Biol. Chem.* **273**, 23086–23092 (1998).

(46) F. Cornelius, N. Turner, and H.R. Christensen, *Biochemistry* **42**, 8541–8549 (2003).

(47) J.C. Skou and M. Esmann, *Methods Enzymol.* **156**, 43–46 (1988).

(48) P. Ottolenghi, *Biochem. J.* **151**, 61–66 (1975).

(49) G.L. Peterson, *Anal. Biochem.* **83**, 346–356 (1977).

(50) O.H. Lowry, N.J. Rosenbrough, A.L. Farr, and R.J. Randall, *J. Biol. Chem.* **193**, 265–275 (1951).

(51) P. Beguin, A.T. Beggah, A.V. Chibalin, P. Burgener-Kairuz, and F. Jaisser, *J. Biol. Chem.* **269**, 24437–24445 (1994).

(52) E.S. Baginski, P.P. Foa, and B. Zak, *Clin. Chem.* **13**, 326–332 (1967).

(53) W. Hug and G. Hangartner, *J. Raman Spectrosc.* **30**, 841 (1999).

(54) T. Miura and G.J. Thomas, Jr., *Subcell. Biochem.* **24**, 55–99 (1995).

(55) K. Hofbauerova, V. Kopecky, Jr, R. Ettrich, M. Kubala, J. Teisinger, and E. Amler, *Biochem. Biophys. Res. Commun.* **306**, 416–420 (2003).

(56) N.M. Gevondyan, E.E. Gavrilyeva, V.S. Gevondyan, A.V. Grinberg, and N.N. Modyanov, *Membr. Cell. Biol.* **9**, 19–26 (1995).

(57) K. Nakamura, S. Era, Y. Ozaki, M. Sogami, T. Hayashi, and M. Murakami, *FEBS Lett.* **417**, 375–378 (1997).

(58) W. Qian and S. Krimm, *Biopolymers* **32**, 1503–1518 (1992).

(59) J.L. Lippert and W.L. Peticolas, *Proc. Natl. Acad. Sci. U.S.A.* **68**, 1572–1576 (1971).

(60) N. Yellin and I.W. Levin, *Biochemistry* **16**, 642–647 (1977).

(61) B.P. Gaber and W.L. Peticolas, *Biochim. Biophys. Acta* **465**, 260–274 (1977).

(62) D.F. Wallach, S.P. Verma, and J. Fookson, *Biochim. Biophys. Acta* **559**, 153–208 (1979).

(63) H.G. Edwards, N.F. Hassan, and A.S. Wilson, *Analyst* **129**, 956–962 (2004).

(64) J.R. Beattie, S. Brockbank, J.J. McGarvey, and W.J. Curry, *Mol. Vis.* **11**, 825–832 (2005).

Circle 47

(65) V. Raussens, M. Pezolet, J.M. Ruysschaert, and E. Goormaghtigh, *Eur. J. Biochem.* **262**, 176–183 (1999).

(66) H.E. Wart, A. Lewis, H.A. Scherag, and F.D. Saeva, *Proc. Natl. Acad. Sci. U.S.A.* **70**, 2619–2623 (1973).

(67) T.J. Gresalfi and B.A. Wallace, *J. Biol. Chem.* **259**, 2622–2628 (1984).

(68) D.F. Hastings, J.A. Reynolds, and C. Tanford, *Biochim. Biophys. Acta* **860**, 566–569 (1986).

(69) A.B. Chetverin and E.V. Brazhnikov, *J. Biol. Chem.* **260**, 7817–7819 (1985).

(70) P.L. Jorgensen, *Biochim. Biophys. Acta* **466**, 97–108 (1977).

(71) P.L. Jorgensen, *Int. J. Biochem.* **12**, 283–286 (1980).

(72) X. Wang, F. Jaisser, and J.D. Horisberger, *J. Physiol.* **491**(3), 579–594 (1996).

(73) C.H. Wu, L.A. Vasilets, K. Takeda, M. Kawamura, and W. Schwarz, *Biochim. Biophys. Acta* **1609**, 55–62 (2003).

Claus Hélix Nielsen can be contacted at Department of Physics, Quantum Protein Centre, Building 309, Office 102,Technical University of Denmark, DK-2800 Lyngby, Denmark.. Tel: +45 45 25 33 30. Fax: +45 45 93 16 69. E-mail: Claus.Nielsen@fysik.dtu.dk

Salim Abdali is with the Quantum Protein Centre, Teechnical University of Denmark, Lyngby, Denmark.

Jens August Lundbaek is with the Department of Physiology and Biophysics, Cornell University, Weill Medical College, New York, NY. **Flemming Cornelius** is with the Department of Biophysics, University of Aarhus, Aarhus, Denmark. ∎